Eurasia Journal of Science and Technology
Print ISSN: 2663-1024
Online ISSN: 2663-1016
DOI: https://doi.org/10.61784/ejst3130

FATIGUE LIFE ANALYSIS OF METRO AXLEBOX BEARINGS BASED ON A VEHICLE-BEARING COUPLED DYNAMICS MODEL

YiFan Yang[1], LinHua Fan[2], ZhengGang Lu[1*]
[1]*School of Transportation, Tongji University, Shanghai 201804, China.*
[2]*Shanghai United Bearing Co.,Ltd, Shanghai 201800, China.*
[*]*Corresponding Author: ZhengGang Lu*

Abstract: Considering the nonlinear characteristics of tapered roller bearings, a coupled dynamic model of a metro vehicle and axle box bearings is established. Based on actual track geometry and train operational schedules, the dynamic force on the axle box bearings are simulated and analyzed under full working conditions, including traction, braking, negotiation of curves with different radii, and straight-line running. The simulation results indicate that compared to traditional vehicle dynamics models, the differences in bearing dynamic force predicted by this coupled model are mainly concentrated above 100 Hz. According to the train operational loads and track characteristics, a full life-cycle dynamic load spectrum for the axle box bearings is constructed. Using this load spectrum and a rolling contact finite element model of the bearing, the dynamic stress spectra at critical nodes of each bearing component are analyzed, followed by an assessment of their fatigue life. The computational results show that, compared to traditional L-P method-based fatigue life calculations using rated dynamic force derived from axle weights, the proposed method—which evaluates bearing fatigue life based on actual application conditions—aligns more closely with reality. This approach can provide more accurate data support for the residual life assessment and maintenance strategy formulation of metro axle box bearings.
Keywords: Metro axlebox bearing; Vehicle-bearing coupled dynamics; Dynamic load spectrum; Fatigue life

1 INTRODUCTION

In recent years, with the high-intensity operation of urban rail transit, the operating environment for metro axlebox bearings has become increasingly complex and demanding. The fatigue life assessment of metro axlebox bearings is integral throughout the entire process of product design, safety assurance, and operation and maintenance decision-making. Traditional simplified models based on rated dynamic loads struggle to accurately reflect the impact of complex dynamic loads encountered in actual metro operations, such as frequent starts/stops and small-radius curves, leading to significant deviations in life predictions. This directly affects the reliability of design and the economics of operation and maintenance. Therefore, constructing a vehicle-bearing coupled dynamics model capable of accurately reflecting time-varying load characteristics becomes key to enhancing the accuracy of life assessment. The prediction of remaining useful life for metro axlebox bearings serves not only as a crucial basis for bearing design and material selection but also as the core foundation for achieving predictive maintenance, optimizing replacement cycles, and ensuring operational safety. It plays an irreplaceable role in improving the whole-life-cycle management level of bearings and operational economic benefits.

Regarding the analysis of bearing dynamic loads, early research primarily obtained them through vehicle dynamics simulations, where bearings were commonly simplified as ideal hinges or rigid connections in the modeling. However, this approach fails to reflect the time-varying stiffness and dynamic contact characteristics within the bearing. Yang Chen et al. further established a bearing-vehicle-track rigid-flexible coupled dynamics model, emphasizing the importance of considering bearing time-varying stiffness and wheel-rail flexibility for load calculation accuracy[1]. Zha et al pointed out that traditional models neglect the dynamic interaction between the wheelset and bearings, thus introducing a multi-degree-of-freedom bearing dynamics model into the vehicle-track coupled model for more realistic simulation of vibration transmission[2,3]. WANG et al., considering nonlinear factors such as bearing time-varying stiffness and clearance, established a vehicle-bearing-track dynamics model to study the influence of wheel polygonization on internal bearing contact loads, revealing that the transmission system affects bearing dynamic characteristics to a certain extent[4,5]. Shi et al. analyzed the evolution of bearing loads under high-frequency wheel-rail excitation through a refined bearing force element model, revealing that the ideal hinge assumption cannot capture the details of load fluctuations[6]. These studies collectively indicate that adopting a vehicle-bearing coupled dynamics model is key to accurately obtaining bearing dynamic loads.

Concerning bearing life prediction, traditional methods based on ISO standards or the Lundberg-Palmgren theory have limited applicability under complex operating conditions. Liu et al. proposed a more conservative life prediction method based on measured loads combined with damage accumulation theory, emphasizing the impact of actual load randomness[7]. Li et al. used Romax to establish a simulation model to obtain contact loads and combined it with the response surface method to optimize bearing structural parameters, thereby improving the safety margin of fatigue

life[8]. Wang et al. employed a monitoring data-driven approach, using dynamic multi-aggregation for remaining useful life prediction, significantly improving prediction accuracy and convergence speed[9]. Meanwhile, Wang et al. studied the impact of electrical erosion stress on bearing life and proposed a correction factor for electrical erosion stress applicable to ISO standards[10]. These advances show that current life assessment is moving towards a refined and dynamic development direction integrating multi-body dynamics simulation, finite element analysis, and data-driven methods.

In this paper, the axle box bearing is integrated as a non-linear force element into the metro vehicle dynamics model. Based on the coupled vehicle-bearing dynamics model, and according to the actual track conditions and train operational schedules, the dynamic loads on the axle box bearings are simulated and analyzed under all operating conditions, including traction, braking, negotiation of curves with different radii, and straight-line running. This enables the construction of a dynamic load spectrum for the axle box bearings, which is subsequently used to perform fatigue life analysis of the bearings.

2 VEHICLE-BEARING COUPLED DYNAMICS MODELING

2.1 Vehicle-Bearing Coupled Dynamics Model

In traditional vehicle system dynamics models, bearings are generally replaced by revolute joints to connect the axle to the axlebox. In constructing the vehicle-bearing coupled model, the core dynamic characteristics of the bearing are centrally embodied through a bearing force element. In the model,a bearing mass body representing the inertial properties of the bearing is first created and connected to the axlebox entity via a force element based on Hertzian contact theory. This force element integrates core physical mechanisms such as nonlinear contact stiffness, damping, radial clearance, and friction inside the bearing, thereby converting the dynamic response from external excitations into forces and moments between the axlebox and the mass body. Through this highly integrated force element, efficient coupling simulation of the bearing's complex nonlinear behavior with the whole-vehicle dynamics system is achieved. Track vehicle-bearing coupled dynamics model based on Simpack is shown in Figure 1.

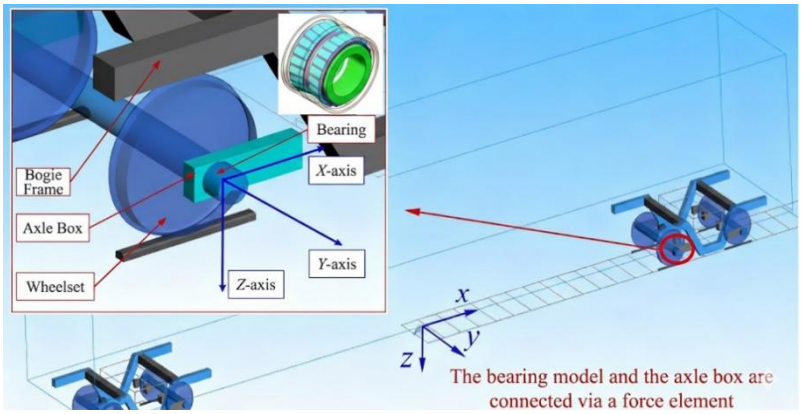

Figure 1 Track Vehicle-bearing Coupled Dynamics Model based on Simpack

The schematic diagram of the contact principle between the roller and the inner/outer raceways is shown in Figure 2. The bearing is subjected to axial load F_a and radial load F_r (Figure 2), causing contact forces on the roller in three directions: the normal contact force Q_e between the roller and the outer raceway, the normal contact force Q_i between the roller and the inner raceway, and the normal contact force Q_f between the roller large end and the inner ring rib. α_e, α_i, and α_f are the contact angles corresponding to these three contact forces. The static equilibrium equation for the contact forces of each roller is:

$$\begin{cases} Q_e \sin\alpha_e - Q_i \sin\alpha_i - Q_f \sin\alpha_f = 0 \\ Q_e \cos\alpha_e - Q_i \cos\alpha_i + Q_f \cos\alpha_f = 0 \end{cases} \tag{1}$$

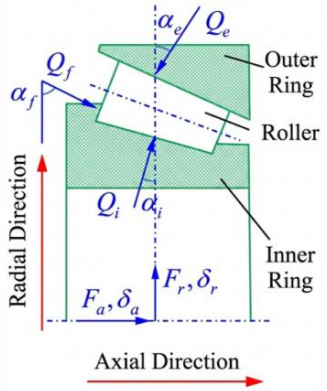

Figure 2 Bearing Contact Schematic Diagram

The normal contact force Q_{ei} between the roller and the outer raceway can be decomposed into a nonlinear elastic force F_{ki} and a damping force F_{di}.

$$Q_{ei}(\delta_{ni}, \dot{\delta}_{ni}) = F_{ki}(\delta_{ni}) + F_{di}(\dot{\delta}_{ni}) \tag{2}$$

The nonlinear elastic force can be obtained according to Hertzian line contact theory, as shown in Equation (3).

$$F_{ki}(\delta_{ni}) = K_{ne} \cdot \delta_{ni}^{10/9} \cdot Sig(\delta_{mi}) \quad , \quad Sig(\delta_{ni}) = \begin{cases} 1 & \delta_{ni} \geq 0 \\ 0 & \delta_{ni} < 0 \end{cases} \tag{3}$$

Where $Sig(\delta_{ni})$is the contact state judgment function for the roller and raceway, with a value of 1 representing contact and 0 representing no contact; K_{ne} is the total contact stiffness between the roller and the outer raceway, related to the contact geometry of the roller and the inner/outer raceways, determined by Equation (4). Equation (4) can be derived from Palmgren's empirical expression [11].

$$K_{ne} = 8.06 \times 10^4 l^{0.89} \left[1 + \left(\frac{\sin(\alpha_e + \alpha_f)}{\sin(\alpha_i + \alpha_f)}\right)^{0.9} \cos(\alpha_e - \alpha_i)\right]^{-1.11} \tag{4}$$

The nonlinear damping force F_d is related to the elastic approach of the roller, and its magnitude behaves differently under different elastic approaches. Its value is calculated by Equation (5) [12],

$$F_{di}(\delta_{ni}, \dot{\delta}_{ni}) = \begin{cases} c(\delta_{ni}, d_c, C_{\max}) \cdot \dot{\delta}_{ni} & , \delta_{ni} \geq 0 \\ 0 & , \delta_{ni} < 0 \end{cases} \tag{5}$$

where c is the damping coefficient; C_{max} is the maximum damping coefficient; d_c is the critical elastic approach. The damping coefficient c is determined by the following equation:

$$c(\delta_{ni}, d_c, C_{\max}) = \begin{cases} C_{\max} & , \ \delta_{ni} \geq d_c \\ C_{\max} - C_{\max} \cdot \Delta^2 \cdot (3 - 2\Delta) & , \ 0 \leq \delta_{ni} < d_c \end{cases} \tag{6}$$

Figure 3 shows the calculation principle diagram for the nonlinear damping force during bearing contact. When bearing are not in contact (δ_{ni}<0), the damping force is 0. When contact begins (δ_{ni}≥0), if the elastic approach is less than the critical elastic approach, the damping coefficient is obtained by cubic spline interpolation, ensuring the continuity of the damping coefficient. If the elastic approach exceeds the critical elastic approach, the damping coefficient reaches the maximum damping coefficient C_{max} and remains constant.

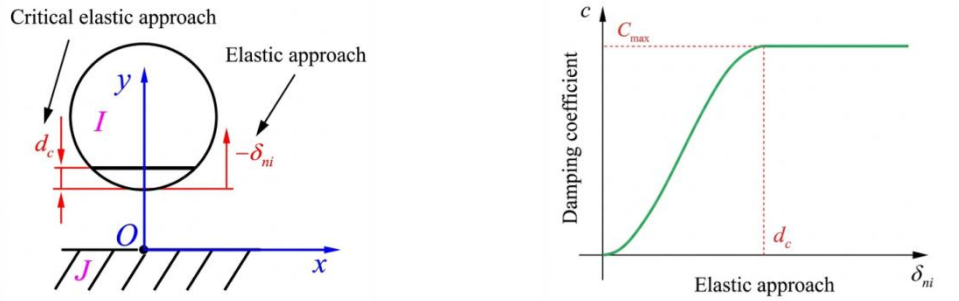

a) Schematic diagram of two objects in contact b) Curve between damping coefficient and elastic approach

Figure 3 Calculation Principle of Contact Nonlinear Damping Force

2.2 Coupled Model Validation

To verify the validity and accuracy of the dynamic force calculation results from the vehicle-bearing coupled model, the differences in bearing dynamic force between the vehicle-bearing flexible coupled dynamics model and the traditional simplified model(the axle box and wheelset are linked by a rotational hinge acting as a bearing substitute) under typical track irregularity excitation are analyzed and compared. Taking a certain metro vehicle as an example, the bearing dynamic force under two conditions are simulated: straight-line running at 120 km/h and braking from 120 km/h to 0. Figure 4 shows the simulation results for the straight-line condition, and Figure 5 shows the results for the braking condition.

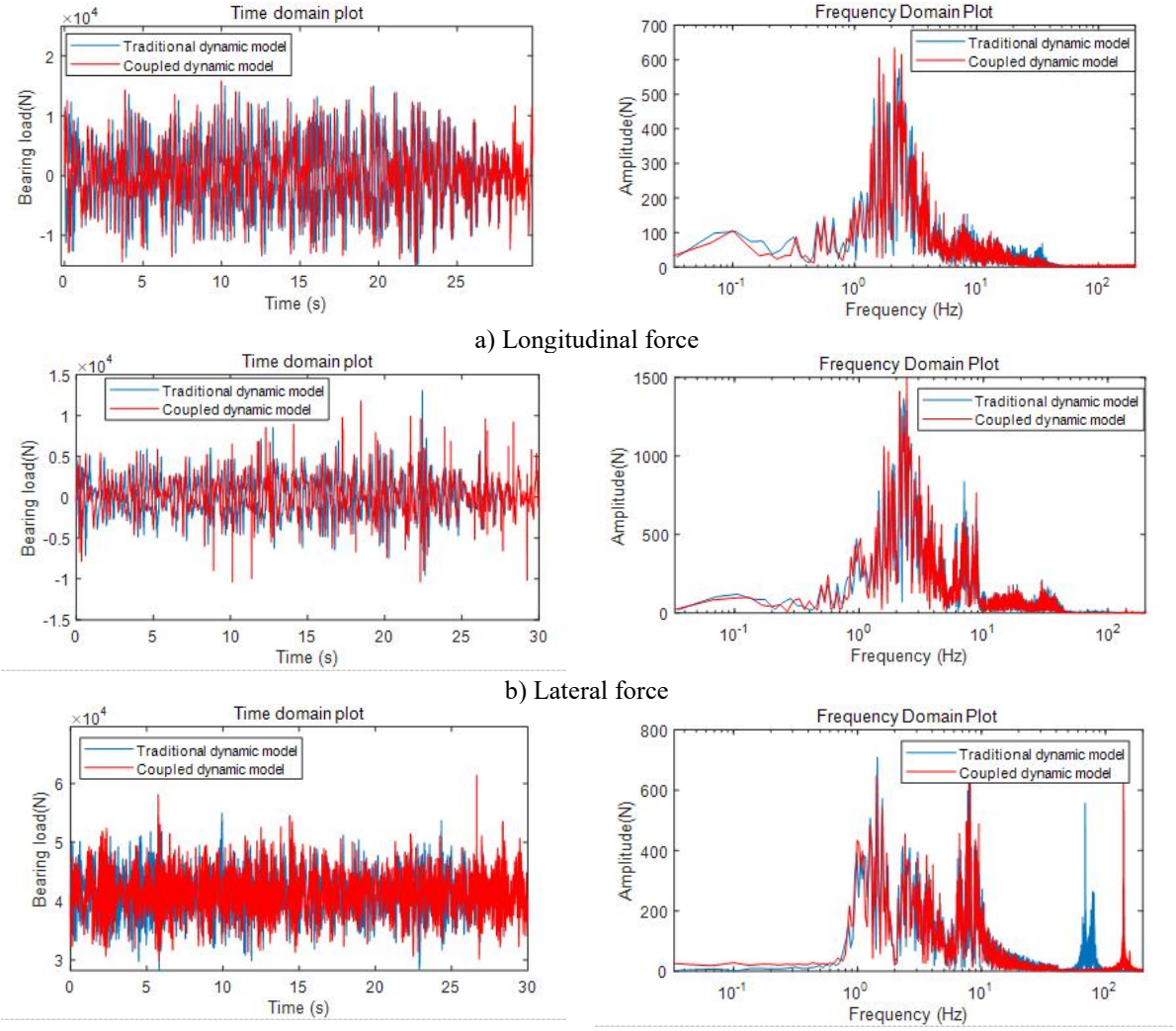

a) Longitudinal force

b) Lateral force

c) Vertical force

Figure 4 Dynamic Force Simulation of Axlebox Bearing under Straight-line Condition

From the straight-line condition, the time-domain wave forms of the force in the three directions calculated using the revolute joint and the coupled dynamics model are essentially consistent, and the frequencies are relatively low. The frequency spectrum analysis diagrams for the longitudinal and lateral force are basically the same. However, in the high -frequency part of the vertical load spectrum, additional spectral peak components appear in the coupled model simulation results that are not reflected in the revolute joint model. These high-frequency components can be attributed to local elastic deformation and nonlinear contact stiffness introduced within the bearing model.

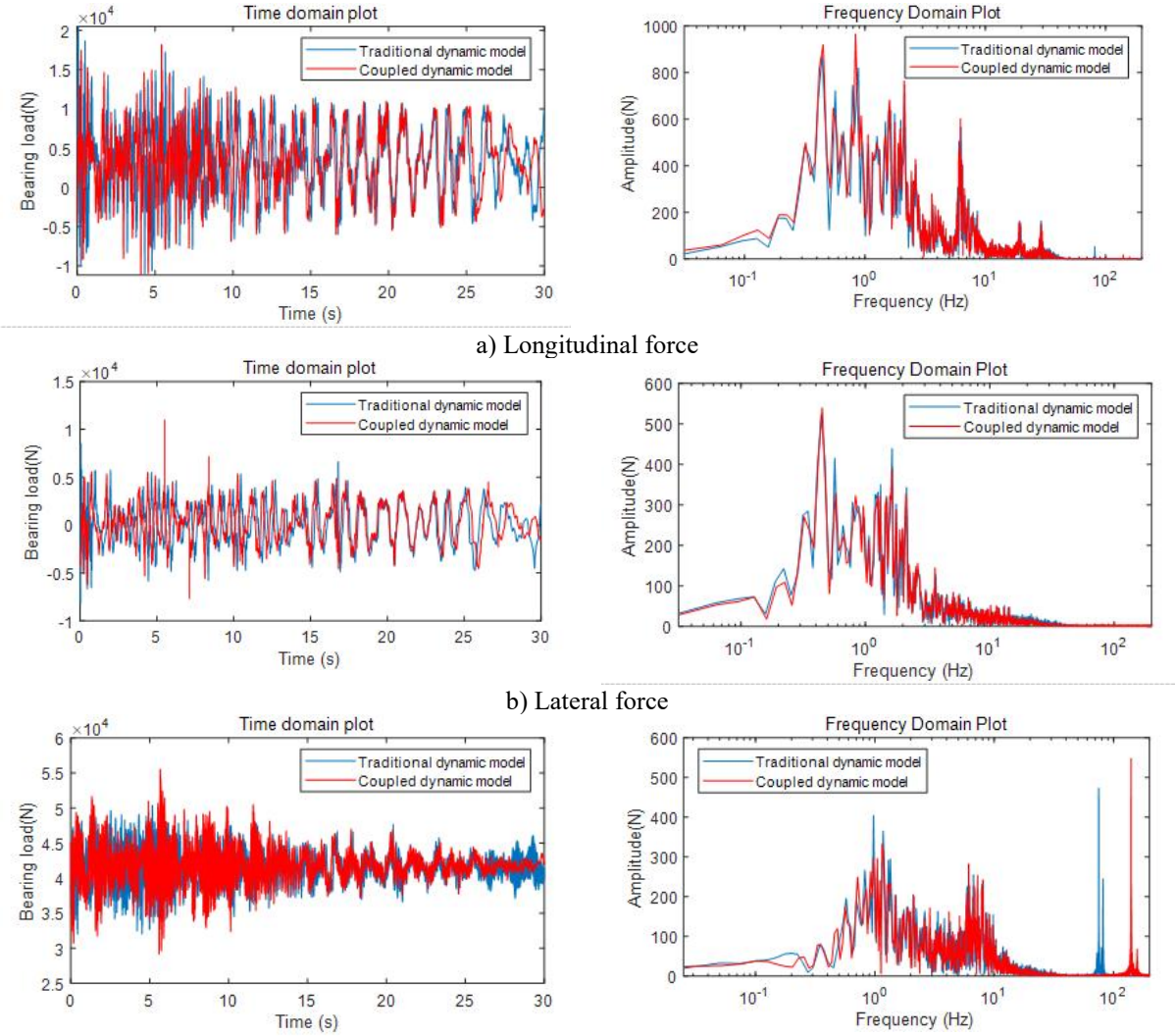

a) Longitudinal force

b) Lateral force

c) Vertical force

Figure 5 Dynamic Force Simulation of Axlebox Bearing under Braking Condition

From the bearing force in the braking condition, it can be seen that although there are some differences in the lateral and longitudinal force, they are generally consistent. Compared to the traditional dynamics model, the coupled dynamics model shows that the vertical force tends to stabilize more as the speed approaches zero, which better conforms to the actual vertical force situation of the bearing at low speeds. In the frequency spectrum, due to the nonlinear characteristics of the bearing under external loads, high-frequency components still exist in the vertical load spectrum of the coupled dynamics model.

3 CONSTRUCTION OF FULL-LIFE-CYCLE LOAD SPECTRUM FOR AXLEBOX BEARINGS

The operational characteristics of metro vehicles include short distances between stations, resulting in frequent braking and traction, as well as numerous curved sections. Meanwhile, metro vehicles frequently load and unload passengers, leading to significant differences in load between peak and off-peak periods. Therefore, when constructing the full-life-cycle dynamic load spectrum for bearings, it is necessary to consider the specific operating line, including straight and curved sections, passenger load conditions, and operational scenarios.

Based on the actual conditions of a studied metro line, considering the operating times and passenger situations during peak and off-peak periods, the load conditions are equivalently categorized into peak load and normal load conditions, with a proposed operating mileage ratio of 1:4. Considering the total line length of approximately 50 km, the longitudinal load on the bearing is larger during traction and braking; while during curve negotiation, the lateral force is larger, and the force on the inner and outer axlebox bearings are inconsistent. The smaller the curve radius, the more severe the condition. According to the line operation diagram, passing an R450m curve with 60mm underbalance represents all curves with radii between R450m and R700m on the entire line; the R800m, 60mm underbalance condition replaces all curves with radii between R800m and R1500m to simulate the most severe condition. For curve radii exceeding 1500m, the straight-line running condition is used instead. The full-life-cycle is simulated through five typical conditions, as detailed in Table 1.

Table 1 Simulation Conditions for Full-life-cycle load spectrum Construction

Condition Type	Condition Parameters
Constant Speed Straight Condition	Running speed: 120 km/h
R450 Curve Condition	Circular curve length: 603 m, Curve radius: 450 m, Passing speed: 95 km/h, Underbalance: 60 mm
R800 Curve Condition	Circular curve length: 463 m, Curve radius: 800 m, Passing speed: 120 km/h, Underbalance: 60 mm
Traction Condition	Speed acceleration from 0 to 120 km/h, Average acceleration: 1 m/s²
Braking Condition	Speed deceleration from 120 km/h to 0, Average deceleration: 0.8 m/s²

The proportion of each simulation condition according to the actual line situation is shown in Table 2.

Table 2 Proportion of Each Condition on the Line

Condition	Constant Speed Straight (%)	R450 Curve (%)	R800 Curve (%)	Traction (%)	Braking (%)
Line Proportion	19.5	17.6	24.6	17.3	21.0

Dynamic simulations are performed for the above five conditions under both peak and normal load situations to obtain the lateral, longitudinal, and vertical dynamic force acting on the axlebox bearing.

During train operation, the axlebox bearing is subjected to longitudinal force F_x, vertical force F_z, and lateral force F_a. F_x and F_z are both radial loads, combined by vector summation. The resultant radial load F_r is:

$$F_r = \sqrt{F_x^2 + F_z^2} \tag{7}$$

When simultaneously subjected to lateral load F_a and radial load F_r, an equivalent radial load P_r is generally obtained using an equivalent method :

$$P_r = XF_r + YF_a \tag{8}$$

Accordingly, the equivalent radial dynamic force for various conditions under normal load are obtained as shown in Figure 6.

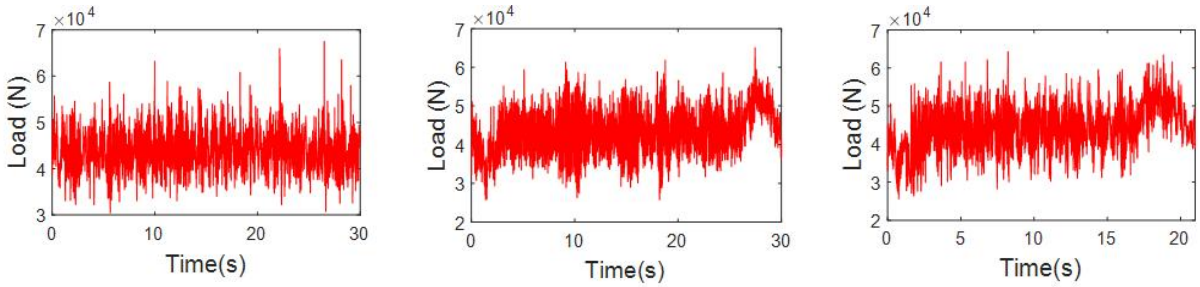

a) Straight condition(v=120 km/h) b) Curve condition 1(R450m) c) Curve condition 2(R800m)

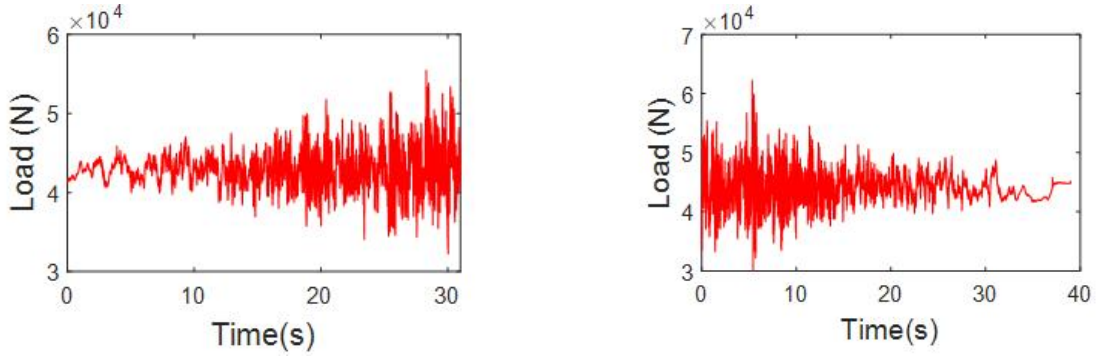

d) Traction condition e) Braking condition

Figure 6 Time History of Equivalent Radial Dynamic Force for Five Conditions under Normal Load

To facilitate fatigue life calculation, the force time histories from each condition are synthesized based on their proportions and sequence, forming a comprehensive dynamic load spectrum for the axlebox bearing representing long-term operational states. The simulated line force for the five conditions (constant speed straight, R600 curve, R800 curve, traction, braking) under both normal and peak load situations are converted to equivalent radial load spectra and then concatenated according to their actual proportion on the line, corresponding to a simulated total line length of approximately 3 km. The constructed equivalent radial force spectra are shown in Figures 7.

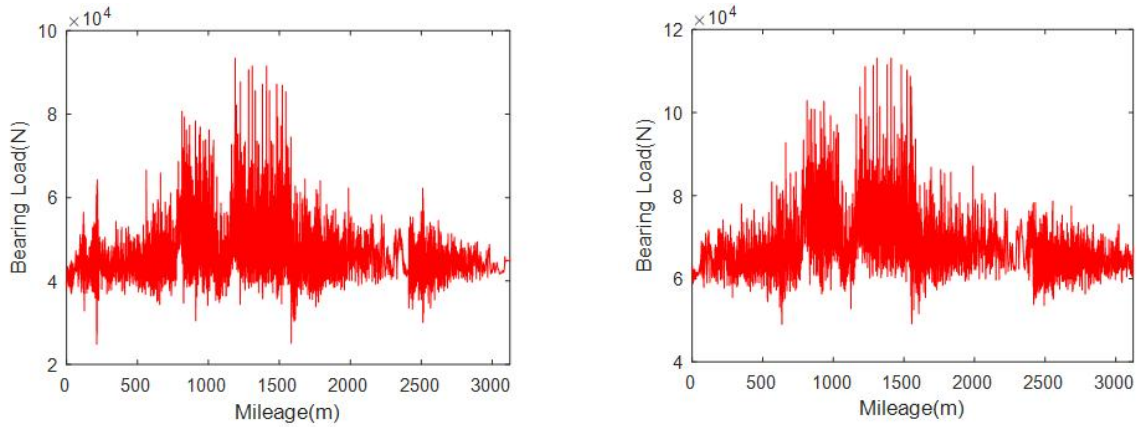

a) Normal load condition b) Peak load condition

Figure 7 Equivalent Radial Load Spectrum

4 FATIGUE LIFE ANALYSIS OF AXLEBOX BEARING

4.1 Bearing Dynamic Stress Analysis

A double-row tapered roller bearing used in a metro axlebox is selected as the research object. Due to the symmetry of the double-row tapered roller bearing, half of the rollers are selected for analysis to improve simulation speed without compromising accuracy, and the loads are also adjusted accordingly. The meshed bearing is shown in the figure. To enhance the calculation accuracy of the bearing finite element model, the mesh in the contact area between the raceways and rollers is refined. The total number of elements is 1,222,485, and the total number of nodes is 1,528,631.

According to the bearing installation, corresponding boundary conditions and constraints are applied to the inner and outer rings. The dynamic stress simulation analysis consists of three steps: first, gravity loading is applied to each bearing component to establish contact between parts; second, loads are applied; finally, rotational speed is applied to the reference point of the inner ring. To reduce the impact of dynamic effects during bearing start-up, both loads and rotational speed are smoothly applied. Using ABAQUS explicit dynamic analysis, a dynamic analysis of the axlebox bearing is performed. Figure 8 shows the von Mises stress contour plots for each component when the equivalent radial load is 26.56 kN and the rotational speed is 600 rpm.

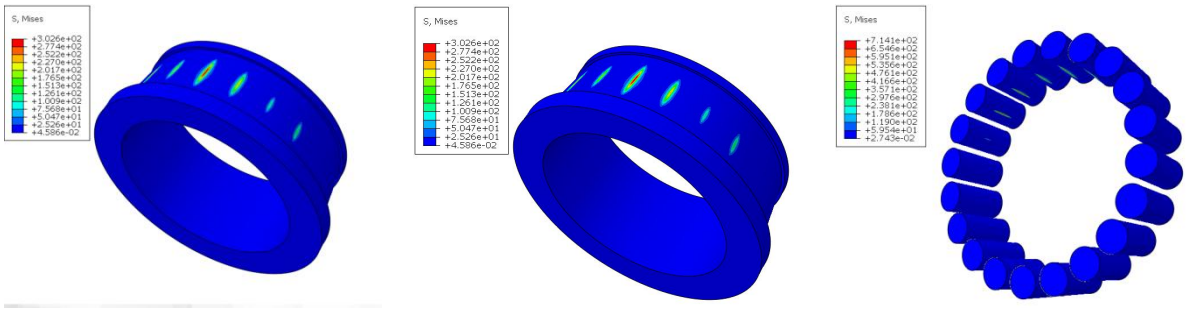

a)Inner ring b)Outer ring c)Roller

Figure 8 Von Mises Stress Contour Plots of Bearing Components

To more precisely analyze the contact stress between the rollers and the inner/outer rings, select node P1 on the outer ring and node P2 on the inner ring, both located within the load-bearing zone, to analyze their stresses at different time steps. The locations of nodes P1 and P2 are shown in the figure 9.

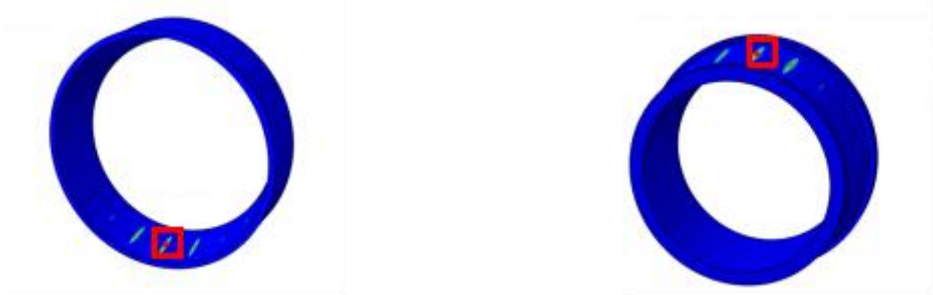

a) Location of outer ring node P1 b) Location of inner ring node P2

Figure 9 Selected Node Locations on Bearing Inner and Outer Rings

The stress-time curves for the bearing outer and inner ring surfaces are shown in Figures 10, respectively. It can be observed that during the entire simulation process, five rollers pass over the node. Under the same inner ring rotational speed, the maximum equivalent stress values when different rollers pass the node are essentially consistent.

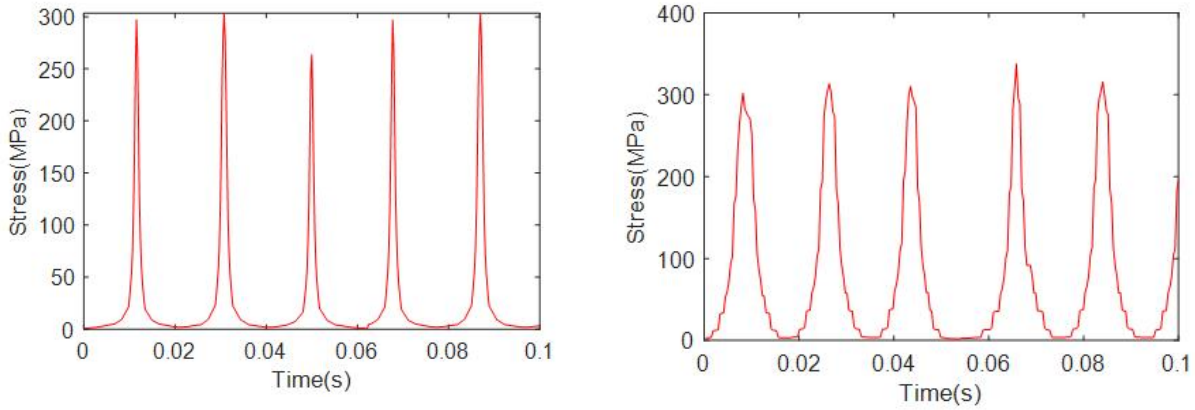

a) Outer ring node P1 b) Inner ring node P2

Figure 10 Node Stress-time Curve

4.2 Fatigue Life Assessment of Axlebox Bearings Based on the Equivalent Dynamic Load Spectrum

This paper employs the Seeger algorithm based on the Fe-Safe fatigue analysis software to calculate the fatigue life of each bearing component. Since the loads on the axlebox bearing constitute a random non-stationary load spectrum, a cycle counting algorithm needs to be introduced to process it before calculating the fatigue damage, followed by correction using the Goodman mean stress correction model. Furthermore, as the stress state in various bearing components is multiaxial, especially at different locations on the bearing, using a uniaxial fatigue assessment method is insufficiently accurate. Therefore, a multiaxial fatigue assessment criterion is required. For multiaxial fatigue analysis of ductile metal components, the Morrow-modified Brown-Miller criterion is generally used.

Based on the dynamic stress simulation analysis of bearing components under rotation for a given equivalent radial load, and integrating the comprehensive equivalent radial load spectrum, the life results for the bearing inner ring, outer ring, and rollers are calculated using Fe-Safe based on the Morrow-modified Brown-Miller multiaxial fatigue criterion, as shown in Figure 11.

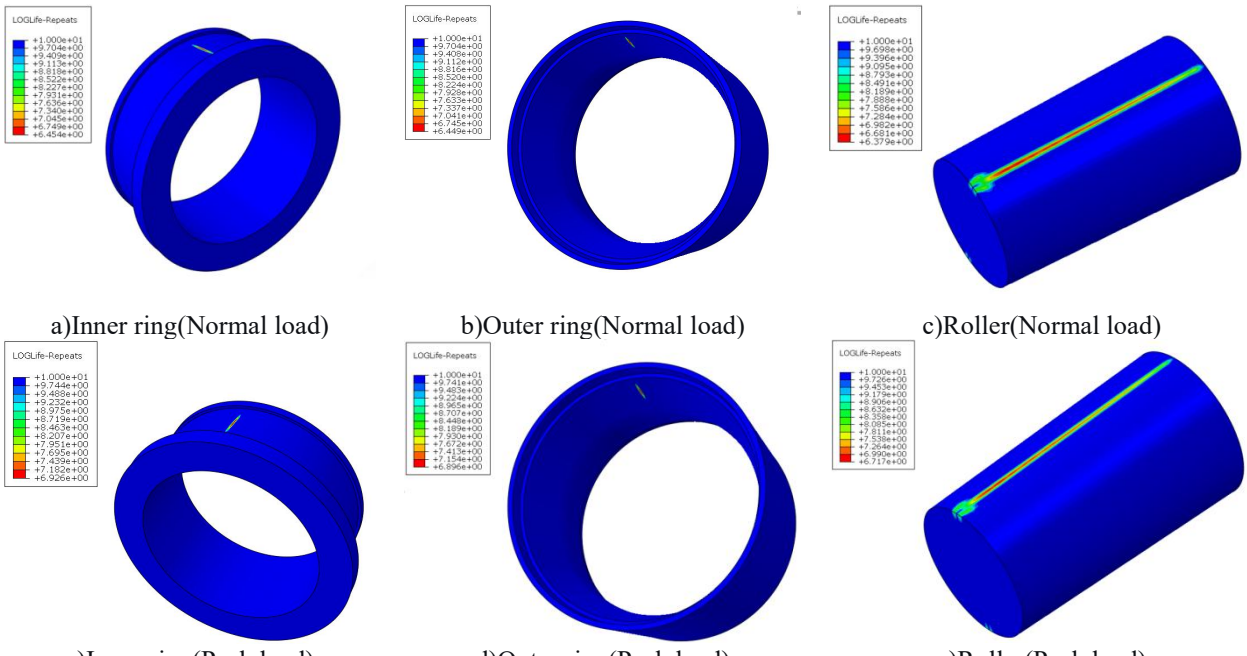

a)Inner ring(Normal load) b)Outer ring(Normal load) c)Roller(Normal load)

c)Inner ring(Peak load) d)Outer ring(Peak load) e)Roller(Peak load)

Figure 11 Logarithmic Life Contours of Axlebox Bearing Components

From the logarithmic life contours of the rollers, inner ring, and outer ring, it can be seen that their critical nodes are all located at the center of the load zone. The rollers have the shortest life. Based on the correspondence between the load spectrum time history and the metro vehicle distance, the fatigue life can be converted into mileage life. The reliability of the S-N curve from conventional metal fatigue tests is 50%. According to the bearing life reliability assessment curve, the bearing fatigue life at 90% reliability is approximately 0.857 times that at 50% reliability. Considering the actual

operating condition ratio of 1:4 between peak load and normal load during metro operation, the life of critical nodes for each bearing component under different conditions is obtained as shown in Table 3.

Table 3 Life of the Most Critical Node for Each Axlebox Bearing Component

Condition	Component	Mileage Life at 50% Reliability (km)	Mileage Life at 90% Reliability (km)
Peak Load Condition	Inner Ring	8.53×10^6	7.31×10^6
	Outer Ring	8.43×10^6	7.22×10^7
	Roller	7.18×10^6	6.15×10^7
Normal Load Condition	Inner Ring	2.53×10^7	2.16×10^7
	Outer Ring	2.36×10^7	2.02×10^7
	Roller	1.56×10^7	1.34×10^7
Actual Operating Condition	Inner Ring	2.11×10^7	1.81×10^7
	Outer Ring	1.98×10^7	1.69×10^7
	Roller	1.35×10^7	1.16×10^7

4.3 Life Analysis and Comparison of Axlebox Bearings Based on the Traditional Lundberg-Palmgren Theory

Based on the axle load, the radial load F_r and the curve axial load F_a are defined as follows:

$$\begin{cases} F_r = K_r \cdot \dfrac{F_o - m_o \cdot g}{2} \\ F_a = k_a \cdot 0.425 \cdot \dfrac{10^4 + \dfrac{F_o}{3}}{2} \end{cases} \tag{9}$$

where K_r=1.2 is the radial load factor, k_a=0.75 is the axial load factor, m_o=1.8 t is the unsprung mass, and F_o=166.6 kN is the axle load.

According to the load combination formula, the equivalent radial dynamic load for straight running P_{r1} is 83.5 kN, and for curve negotiation P_{r2} is 109.9 kN. From Table 2, the proportion of curve conditions is 42.2% and straight conditions is 57.8%. Thus, the equivalent dynamic load is calculated as:

$$P_r = \sqrt[\frac{10}{3}]{0.422 \times P_{r1}^{\frac{10}{3}} + 0.578 \times P_{r2}^{\frac{10}{3}}} = 100.69\ \text{kN} \tag{10}$$

The basic dynamic force rating of this bearing C_r is 961.93 kN. Taking the semi-worn diameter D_r= 805 mm, the bearing mileage life L_{10s} is:

$$L_{10s} = 2.5 \times 10^3 \times \left(\frac{C_r}{P}\right)^{\frac{10}{3}} = 4.62 \times 10^6\ \text{km} \tag{11}$$

At a 90% reliability level, the fatigue life of the metro axle box bearing calculated based on the simulated equivalent dynamic load spectrum is approximately 11.6 million kilometers, whereas the result derived from the classical L-P theory is about 4.62 million kilometers, indicating a significant discrepancy between the two. In fact, the L-P theory-based method for calculating axle box bearing life adopts the fatigue life under the most severe AW3 load condition. However, the actual load on metro vehicles varies with peak and off-peak hours and is generally lower than the AW3 condition. Therefore, the result based on the L-P theory tends to be conservative.

In contrast, the analysis method proposed in this paper comprehensively considers the distance proportions of various typical operating conditions in actual lines—such as curves, straight sections, traction, and braking—as well as the temporal load variations between peak and off-peak hours during service. This enables a more realistic reconstruction of the multiaxial, variable-amplitude loading history. The dynamic load spectrum for the axle box bearing constructed accordingly, along with the fatigue life assessment, can more reasonably reflect the fatigue damage of the bearing under complex full-range operating conditions on this specific metro line, leading to more accurate life prediction. This approach helps identify the contribution of different operating phases and conditions to bearing damage, while significantly enhancing the accuracy and credibility of life prediction.

5 CONCLUSION

Based on the coupled vehicle-axle box bearing dynamics model and the actual route data of a metro line, this study constructs a full-life cycle load spectrum for the bearing. Fatigue life analysis is then conducted using this load spectrum, and the results are compared with those obtained from the traditional L-P theory. The main conclusions are as follows:

1.This paper proposes a method for analyzing the radial and axial dynamic loads on axle box bearings throughout their entire life cycle by establishing a coupled dynamics model of metro vehicles and axle box bearings, combined with actual operating routes, loads, and application scenarios such as straight-line running, curved tracks of different radii, traction, and braking. Compared with simplified models that replace bearings with traditional rotational hinges, this method can analyze the highly coupled characteristics between the complex nonlinear dynamic behavior of bearings

and the vehicle dynamics system, enabling more accurate analysis of axle box bearing dynamic loads and supporting bearing life assessment under specific metro line conditions.

2.A finite element model for rolling contact was developed for the double-row tapered roller bearings commonly used in metro axle boxes. Based on the obtained dynamic load spectrum of the bearings over their full life cycle, the dynamic stress calculation and fatigue life of critical nodes in each bearing component were analyzed. For the specific route, vehicle, and axle box bearing parameters analyzed, with 90% reliability, the fatigue life of the rollers is approximately 11.6 million kilometers. Compared with the traditional L-P method, the approach adopted in this paper comprehensively considers actual routes, loads, and operating conditions, resulting in a more accurate calculation of bearing fatigue life.

It should be noted that the construction of the dynamic load spectrum for axle box bearings currently primarily considers five typical route conditions. However, during metro vehicle operation, special situations such as wheel out-of-roundness, tread flats, passage over rail joints, and turnouts may occur, which induce significant impact loads on axle box bearings and affect their fatigue life. Future work will further analyze the impact loads on axle box bearings under these special conditions, providing a more accurate analytical model and data support for axle box bearing design and life assessment. Additionally, a dynamic load measurement device for axle box bearings will be developed to validate the simulation analysis model and promote data-driven residual life assessment and intelligent maintenance of in-service metro vehicle axle box bearings.

COMPETING INTERESTS

The authors have no relevant financial or non-financial interests to disclose.

FUNDING

This research was sponsored by the Explorers Program of Shanghai (Grant No. 24TS1416300).

REFERENCES

[1] Yang Chen, Chi Maoru, Wu Xingwen, et al. Dynamic load calculation method for EMU axle box bearings based on vehicle dynamics. Journal of Mechanical Engineering, 2023, 59(14): 179-189.

[2] Zha Hao, Ren Zunsong, Xu Ning. Vibration performance of high-speed vehicles with axlebox bearing. Journal of Mechanical Engineering, 2018, 54(16): 144-151.

[3] Zha Hao, Ren Zunsong, Xu Ning. Load characteristics of axlebox bearing raceway of high-speed EMU. Journal of Mechanical Engineering, 2020, 56(4): 135-142.

[4] Wang Zhiwei, Allen Paul, Mei Guiming, et al. Influence of wheel-polygonal wear on the dynamic forces within the axle-box bearing of a high-speed train. Vehicle System Dynamics, 2020, 58(9): 1385-1406.

[5] Wang Zhiwei, Zhang Weihua, Yin Zhonghui, et al. Effect of vehicle vibration environment of high-speed train on dynamic performance of axle box bearing. Vehicle System Dynamics, 2019, 57(4): 543-563.

[6] Shi Huailong, Zhou Junyi, Wang Yong, Chen Longfei. Analysis of load characteristics of axlebox bearings under high-frequency wheel-rail excitation of high-speed EMU. Journal of Vibration and Shock, 2025, 44(19): 248-256.

[7] Liu Dekun, Li Qiang, Wang Xi, et al. Life prediction method for EMU axlebox bearings based on measured loads. Journal of Mechanical Engineering, 2016, 52(22): 45-54.

[8] Li Zhihua, Huang Zhihui, Tang Jiacheng, et al. Optimization of axlebox bearing structural parameters based on response surface method and simulation calculation. Railway Locomotive & Car, 2025, 45(02): 86-94.

[9] Wang Biao, Qin Yong, Jia Limin, et al. Monitoring data-driven remaining useful life prediction for urban rail train axlebox bearings. Journal of Southwest Jiaotong University, 2024, 59(01): 229-238.

[10] Wang Liguo, Qu Tianwei, Qu Song, et al. Research on key issues affecting the reliability of bearings in inverter-fed drive units. Railway Locomotive & Car, 2023, 43(05): 127-134.

[11] Palmgren, A. Ball and roller bearing engineering. Burbank, Philadelphia, 1959.

[12] Lankarani H M, Nikravesh P E. Continuous contact force models for impact analysis in multibody systems. Nonlinear Dynamics, 1994, 5, 193-207.